J Clust Sci (2017) 28:2919–2932
DOI 10.1007/s10876-017-1270-5

ORIGINAL PAPER

Evaluation of the Anticoagulant and Catalytic Activities of the *Bridelia retusa* Fruit Extract-Functionalized Silver Nanoparticles

Ramesh Vinayagam[1] · Thivaharan Varadavenkatesan[1] · Raja Selvaraj[1]

Received: 17 June 2017 / Published online: 15 July 2017

Abstract An eco-friendly, green synthesis of silver nanoparticles (SNPs) employing the fruit extract of *Bridelia retusa* was investigated. The UV–visible spectrum showed the surface plasmon peak at 436 nm, a characteristic feature of SNPs. SEM image showed spherical nanoparticles and EDX evidenced the presence of metallic silver with a strong signal for silver atoms at 2.98 keV. XRD patterns verified the crystalline nature of the SNPs which depicted a sharp peak at 38.52° corresponding to (111) plane and the average crystallite size was determined as 22.48 nm. Fourier Transform Infrared spectroscopic analysis confirmed the role of phenolic compounds in the synthesis and stabilization of nanoparticles. The average hydrodynamic diameter of the nanoparticles was 68.49 nm and their polydispersity index was 0.171 which corroborated the monodispersity. A high negative zeta potential value (−27 mV) provided the stability to the colloidal nanoparticle solution. The accelerated reduction of the Congo red dye in the presence of SNPs with a degradation rate constant of 0.056 min^{-1} confirmed the catalytic potential of nanoparticles. Moreover, the synthesised nanoparticles inhibited the formation of blood clots in human blood samples which proved the anticoagulant activity and hence the nanoparticles can be used in nanomedicine.

Keywords *Bridelia retusa* · Silver nanoparticles · Congo red · Dye degradation · Anticoagulants

✉ Raja Selvaraj
rajaselvaraj@gmail.com

[1] Department of Biotechnology, Manipal Institute of Technology (MIT), Manipal University, Manipal, Karnataka 576104, India

Introduction

In recent times, the research in the area of metallic nanoparticles has attracted many scientists because of their improvised specific properties as compared to their respective bulk state. To be specific, silver nanoparticles (SNPs) have profound applications in various areas such as anticancer [1], antibacterial, antioxidant [2], anticoagulant [3], larvicidal [4], enzyme stability [5], biosensors [6], dye removal [7] and petroleum hydrocarbon removal [8]. These versatile applications, undoubtedly made the SNPs as one of the emerging areas in the field of nanoparticle research [9].

There are many traditional physical and chemical methods of synthesis of metallic SNPs available. However, these methods involve the usage of high energy input and toxic chemicals. But, now-a-days, there is an ongoing demand for a non-toxic, eco-friendly and cost-effective synthesis method of nanoparticles.

Plant-mediated synthesis method is one of such methods which addresses all the limitations of the traditional synthesis procedure. The plant-mediated synthesis method is "cost-effective" (employs only agricultural waste materials such as leaves, fruits, stems and roots), and "green" (does not necessitate any harmful chemicals) method. In addition, the synthesis procedure is rapid and does not require high temperature or pressure.

The various inherent biomolecules of the plant extract play the dual function of formation and stabilization of SNPs. This is an additional advantage of plant-mediated synthesis because a separate stabilization agent should be added in the conventional chemical synthesis method.

Very recently, many articles for the synthesis of SNPs by plant-mediated green synthesis have been reported. *Physalis angulate* [2], *Salvadora persica* [7], *Syzygium aromaticum* [1], *Cordia dichotoma* [10], *Amaranthus gazngeticus Linn* [11], *Lippia citriodora* [4], *Convolvulus arvensis* [12], *Salvia miltiorrhiza* [13] and *Atrocarpus altilis* [14] to name a few.

Bridelia retusa is a moderate sized tree which belongs to *Euphorbiaceae* family found in Asian countries, particularly in the hotter parts of India [15]. Various parts of this tree have been used in the folk medicine traditionally. It is reported that the *B. retusa* fruits are rich in gallic acid, ellagic acid, β-sitosterol and tannins [16]. The presence of these polyphenolic phytoconstituents ascribed for the antinociceptive and anti-inflammatory potential of the methanolic extract of *B. retusa* fruit extract as demonstrated by [17]. We propose that these biomolecules could play a vital role in the synthesis and stabilization of SNPs.

The research group [18] was the first to publish an article on the synthesis of SNPs using *B. retusa* leaf extract. Nevertheless, to the best of our knowledge, there are no reports available in the literature for the synthesis of SNPs using the *B. retusa* fruit extract. Therefore, the current investigation aims at the synthesis of SNPs using the aqueous extract of *B. retusa* fruit and characterization by various methods. In addition, the catalytic activity to degrade a pollutant dye, Congo red (CR) and the anti-coagulant potential to prevent blood coagulation by the SNPs were also investigated.

Materials and Methods

Materials

Silver nitrate was obtained from Merck, India. The fresh fruits from *B. retusa* tree were harvested during the month of February in MIT campus, Manipal University.

Preparation of Aqueous Fruit Extract of *B. retusa*

The fresh *B. retusa* fruits (Fig. 1) were completely cleaned (surface washed and rinsed with Milli-Q water) and then air dried for 4–5 h at room temperature. 5 g of fruits were added to 50 mL of Milli-Q water in a beaker and boiled at 80 °C for 20 min. Filtration was done after bringing down the contents to room temperature. A clear pale-brown color filtrate was collected and designated as *B. retusa* fruit extract (BRFE) which was preserved in the refrigerator for further synthesis procedure.

Synthesis of SNPs

5 mL of BRFE was mixed with 45 mL of 1 mM of $AgNO_3$ solution in a beaker and kept in a thermostat at 80 °C for 10 min. The color of the beaker contents changed to golden-brown which indicated the formation of SNPs. The purified SNPs were obtained by centrifuging the colloidal solution thrice at 8000 rpm for 10 min with concomitant re-dispersion of pellet with Mill-Q water in each step.

Fig. 1 Fruits of *Bridelia retusa* tree used in this study

Characterization of SNPs

UV–Vis spectroscopy was employed to monitor the synthesis of SNPs. For this purpose, a known amount of colloidal suspension was properly diluted with Milli-Q water in a quartz cuvette and spectra was analysed using UV–Vis spectrophotometer (Shimadzu) with a resolution of ±1 nm. The surface morphology of a thin film of SNPs was analysed by Scanning Electron Microscope (EVO MA18) and the elemental composition was examined through energy dispersive X-ray (EDX) analysis. The reactive groups of phytochemicals present in BRFE may probably involve in the protection of SNPs surface by capping action which was analysed by Shimadzu-8400S spectrophotometer. The FTIR spectra of SNPs were taken by mixing the dried nanoparticles with KBr to form pellets. The transmittance of the pellets was measured in the range from 4000 to 400 cm^{-1}. The crystallite structure of the SNPs was obtained by drop-casting the colloidal suspension on to a glass slide and XRD pattern was analysed using an X-ray diffractometer (Rigaku Miniflex 600). The hydrodynamic size of SNPs and zeta-potential of the colloidal suspension were estimated by dynamic light scattering method (Malvern Zetasizer nanosizer).

Anticoagulant Activity

This study was performed according to the procedure given in our earlier report [19]. In this procedure, fresh human blood sample was collected from a healthy person in two separate glass vials. One of the vials was used as a control (without SNPs) and another one was added with 0.5% (v/v) freshly prepared SNPs to examine the anticoagulation property. The formation of blood clots in both vials was monitored visually for a specific duration of time with vigorous mixing of the vials at room temperature.

Catalytic Activity of SNPs

The catalytic potential of the synthesised SNPs for the reduction of a pollutant dye—Congo red, by sodium borohydride solution was examined. A known concentration of dye solution was taken in two clean cuvettes and 200 µL of $NaHB_4$ was added. The first cuvette was used as negative control and 200 µL of SNPs was added to the second cuvette. After thorough mixing, absorbance of both samples at a λ_{max} 498 nm was monitored for a specific time duration using UV–Vis spectrophotometer.

Results and Discussions

Visual Observation

The Fig. 2a–c show the color of the silver nitrate, BRFE and SNPs respectively. The change in color of the reaction mixture from pale-brown to brownish golden appearance indicated the synthesis of SNPs. The formation of brownish golden

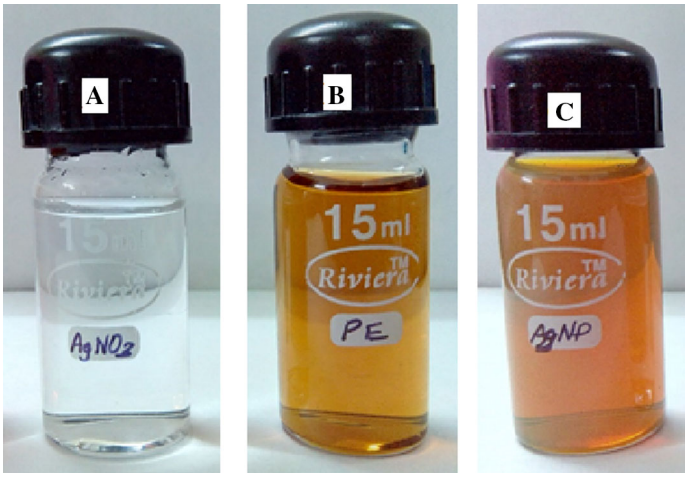

Fig. 2 Formation of SNPs using the fruit extract of *Bridelia retusa*. **a** Silver nitrate, **b** BRFE and **c** SNPs

color is one of the characteristic features of SNPs as evidenced by many published reports [20–22]. The change in color is due to the reduction of the silver metal ion (Ag^{+}) to SNPs (Ag^{0}) by the phenolic compounds present in the BRFE as mentioned in the "Introduction" section.

UV–Vis Spectroscopy

UV–Vis spectroscopy is one of the powerful methods to verify the formation of SNPs. The formation of brownish golden color is attributed to the excitation of surface plasmon resonance (SPR) which depends on the size and shape of the nanoparticles, the type of reducing agent and the concentration of precursors used. According to [23], the color change and the occurrence of SPR are due to the collective oscillation of electrons in the conduction band which will be indicated in the visible region of the spectrum. In general, SNPs show a specific SPR peak in the range of 400–480 nm [24]. In the present study, a well-defined SPR band was observed at 436 nm (Fig. 3) which is the characteristic absorption band for SNPs. Similar results were reported by [25, 26] for the green synthesis of SNPs using *Azadirachta indica* aqueous leaf extract and *Zisiphus spina-christi* extract respectively. The single-broad band obtained in this work may be attributed to the formation of spherical shaped nanoparticles as explained by [27] for the synthesis of SNPs using *Ficus carica* fruit extract.

SEM and EDX

The SEM image of the synthesised SNPs is shown in the Fig. 4. Both individual and aggregates of nanoparticles can be noticed in the image. The aggregate formation may be because of the procedures involved in the sample preparation [28]. The

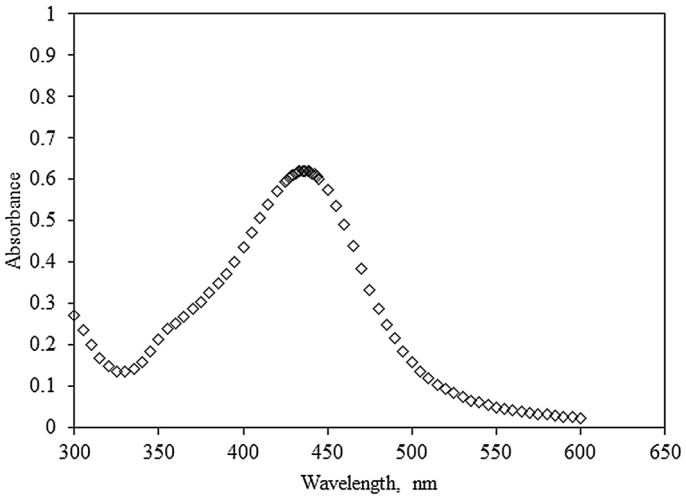

Fig. 3 UV–Vis spectra of SNPs synthesised using the fruit extract of *Bridelia retusa*

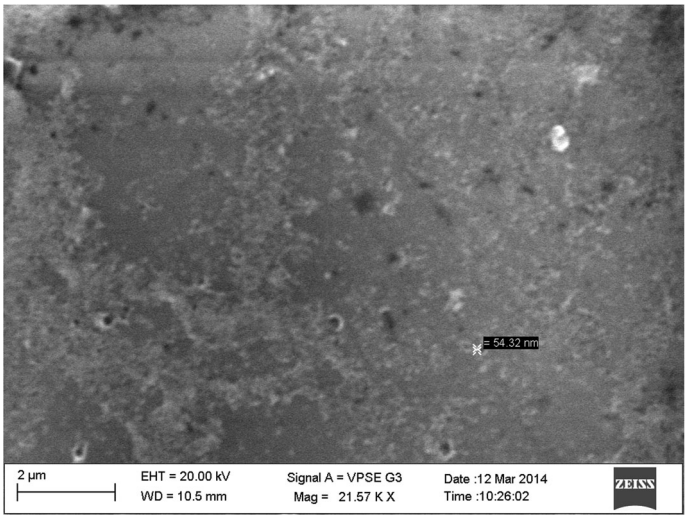

Fig. 4 SEM image of the SNPs synthesised using the fruit extract of *Bridelia retusa*

individual nanoparticles are spherical in shape and the size of one of such spherical shaped nanoparticles (54.32 nm) is shown in the image.

In EDX (Fig. 5), a strong signal for silver atoms at 2.98 keV was observed. Apart from silver, there were other peaks such as Na, Si and Ca which were believed to be risen from the glass slide which held the thin film of sample for analysis as documented by [29–31].

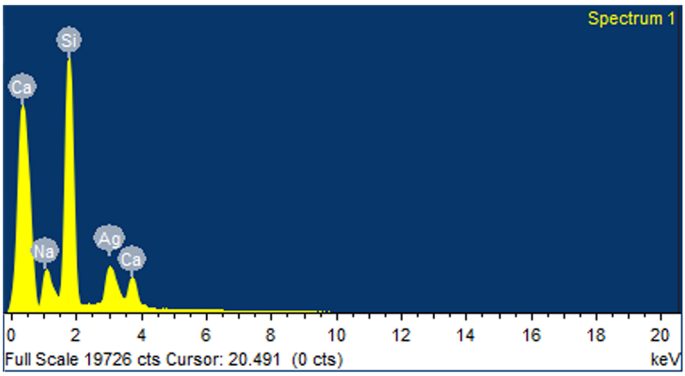

Fig. 5 EDX spectrum of SNPs synthesised using the fruit extract of *Bridelia retusa*

XRD Analysis

The crystal structure of the synthesised SNPs was elucidated by XRD analysis (Fig. 6). The XRD pattern portrayed four peaks at 2θ values of 38.52°, 44.73°, 65.02° and 77.82° which corresponded to the Bragg reflections from (111), (200), (220) and (311) respectively. These reflections substantiate the face-centered-cubic crystal structure of metallic SNPs. Similar kind of results has been obtained by [32] for the synthesis of SNPs from the rhizome extract of *Curculigo orchioides* Gaertn. and by [12] for the *Convolvulus arvensis* extract functionalized SNPs. The sharp peak at 38.52° depicted the dominance of (111) plane.

The interplanar spacing and lattice parameter values were calculated as 0.2335 nm and 0.4045 nm respectively, which were coherent with the standard powder diffraction file (JCPDS, No. 04-0783) [14]. The crystallite size of the nanoparticles was calculated as 22.48 nm by Debye–Scherrer equation [33], which ascertained the nano size of the SNPs.

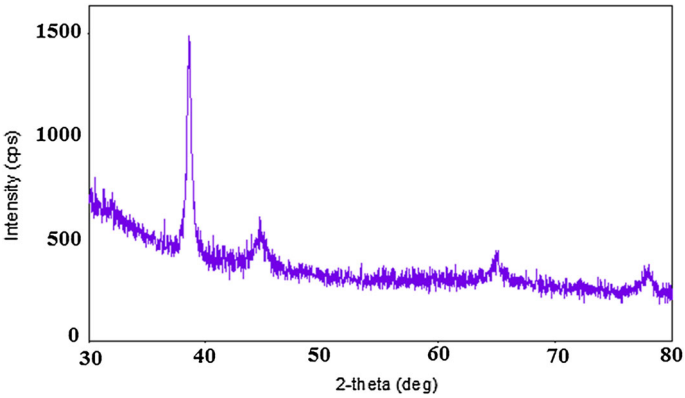

Fig. 6 XRD pattern of SNPs synthesised using the fruit extract of *Bridelia retusa*

FTIR

FTIR spectrum (Fig. 7) is used to ascertain the role of specific functional groups present in the BRFE for the formation and stabilization of SNPs. The fruit extract mediated SNPs shows broad bands at 3571.92 and 3402.20 cm^{-1} which correspond to O–H stretching of carboxylic group and alcohol respectively [34]. The double bands at 2931.60 and 2885.31 cm^{-1} indicate the C=H stretching of methylene groups [21]. The sharp absorption band at 2352.99 cm^{-1} indicates the S–H vibration of L-cysteine, which ascertained the stabilization of SNPs by the L-cysteine present in the BRFE. This finding is identical to our earlier reports [19, 35].

The medium band at 1596.95 cm^{-1} corresponds to N–H bending vibrations of amine functional groups. The weak band at 1728.10 cm^{-1} links to C=O stretching vibrations of carboxylic acids or esters. The symmetric stretching vibration of carboxyl group was observed at 1450.37 and 1388.65 cm^{-1} [26]. The broad bands between 1072.35 and 1010.63 cm^{-1} endorse the C–O stretching vibration of flavonoids present in the fruit extract [4]. It can be evinced from these bands that presence of hydroxyl, amino, carbonyl, carboxyl and sulfhydryl groups present in the fruit extract might be responsible for the formation and stabilization of SNPs.

DLS Studies

With the objective to determine the size, the size distribution and the stability of the nanoparticles synthesised, the DLS studies were done. The distribution of the size of the SNPs is depicted in the Fig. 8. The graph shows the various sizes of the nanoparticles ranging from 28.21 to 141.8 nm and more than 40% of the particles were within 40 nm range. However the average particle size was 68.49 nm which ascertained the nano range of the nanoparticles. Similar kind nanoparticle size (less than 100 nm) has been obtained by [36] for the synthesis of SNPs using the latex of *Jatropha gossypifolia* and *J. curcus* and by [37] using the culture supernatants of *Enterobacteria*.

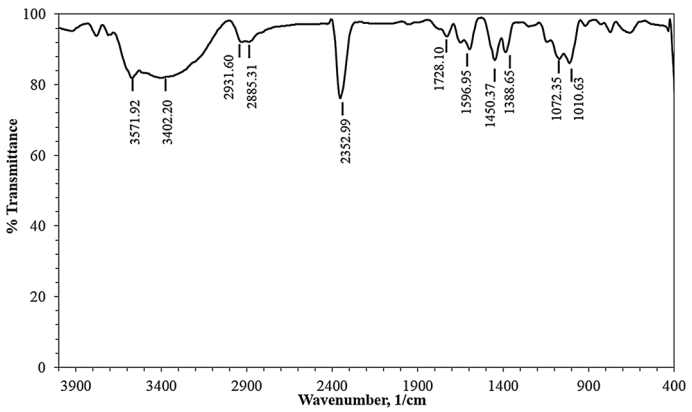

Fig. 7 FTIR spectrum of SNPs synthesised using the fruit extract of *Bridelia retusa*

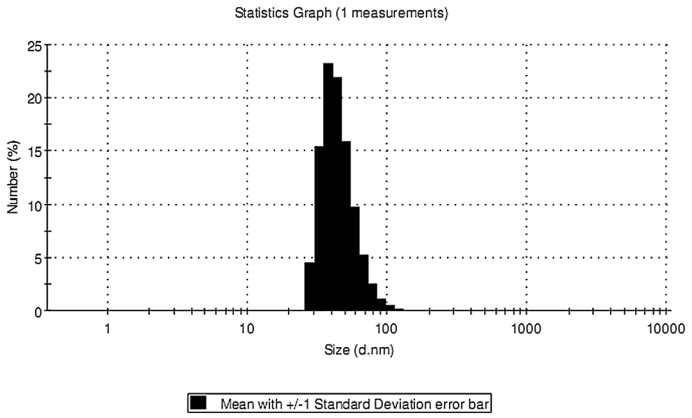

Fig. 8 Particle size distribution of SNPs synthesised using the fruit extract of *Bridelia retusa*

The uniformity and the homogeneity of the nanoparticles are indicated by a parameter called polydispersity index (PDI) and a value of less than 0.2 is preferred for monodispersity. In the present study, the PDI was 0.171 which substantiated the monodispersity of the nanoparticles synthesised [38].

Zeta potential is the measure of the stability of SNPs. The literature [39] suggests that the solutions with zeta potential above +25 mV or below −25 mV will have more stability. In our present study, a zeta potential value of −27 mV was obtained (Fig. 9) which affirmed the stability of the nanoparticles [38]. The high negative value provides the repulsion between the particles and provides a stable solution without any aggregation. The results are coherent with the SNPs synthesised using *Cinnamon zeylanicum* bark extract [40].

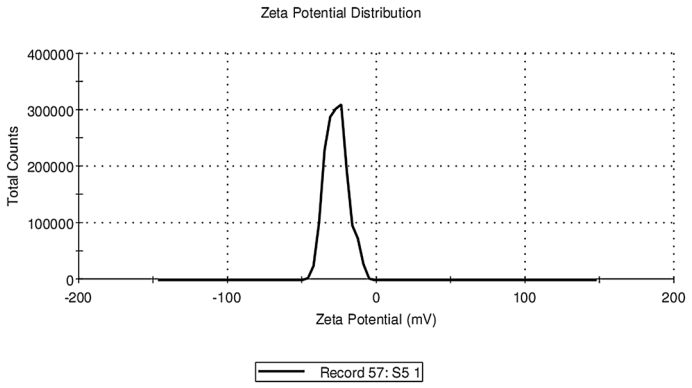

Fig. 9 Zeta potential distribution of SNPs synthesised using the fruit extract of *Bridelia retusa*

Anticoagulant Activity

The anticoagulant activity of SNPs on human blood sample is presented in Fig. 10. The vial with SNPs (A) did not show any blood clots whereas the control vial B (without SNPs) formed blood clots within 5 min.

We monitored the vial A for more than a month and did not witness any blood clot formation. The inhibition of blood clot formation by SNPs corroborates the anticoagulant activity of the synthesised SNPs. The findings are in accordance with the published literature [12]. The prevention of coagulation of blood may be due to the inhibition of aggregation of platelets by the SNPs, as explained by [41]. The inhibition of fibrinogen and platelet aggregation were responsible for the anticoagulant activity of SNPs [3]. The results clearly suggest that the SNPs synthesised by this method can be used as anticoagulant for the treatment of blood coagulation disorders in the field of nanomedicine.

Catalytic Activity of SNPs

CR dye is a secondary diazo anionic dye which is widely used in textile industries. The effluents containing CR dye have low biological and chemical oxygen demands which pose an environmental threat [42]. In order to degrade this pollutant dye, an eco-friendly method using SNPs has been attempted. In this method, the catalytic activity of the SNPs was evaluated by the degradation of CR dye in the presence of $NaBH_4$. It can be visualised from Fig. 11 inset that the intense red color of the reaction mixture containing SNPs faded and became colourless at the end of the catalytic process.

The UV–Vis spectra of CR degradation in the presence of SNPs show maximum absorption band near 495 nm. The intensity of the absorbance of CR dye decreased continuously which is attributed to the degradation of the dye. The degradation process was completed within 24 min in the presence of SNPs. However, there was no significant change in the absorbance of the sample without SNPs and the reduction was very less (data not shown). This substantiates the importance of the presence of SNPs for the catalytic degradation of the CR dye. It is documented that the SNPs catalyse the reduction of the dye by facilitating the electron relay from BH_4^- to CR dye [43]. The degradation of dye may be due to the excitation of

Fig. 10 Anticoagulant activity of SNPs synthesised using the fruit extract of *Bridelia retusa*. **a** Blood sample with SNPs. **b** Blood sample without SNPs

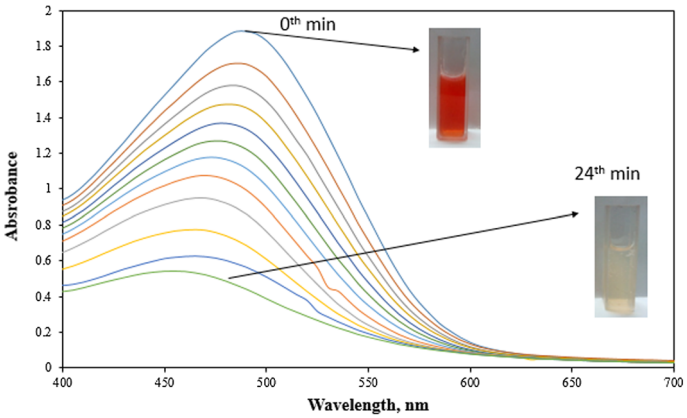

Fig. 11 Sequential UV–Vis spectra of degradation of CR dye in the presence of $NaBH_4$ and SNPs

surface electrons and their interaction with the dissolved oxygen molecules and concomitant production of hydroxyl radicals, thus allowing silver ion interactions with the dye molecule [10].

The rapid reduction of the CR dye in the presence of SNPs is due to the smaller size and the larger surface area of the synthesised nanoparticles. The degradation process was modelled according to the following pseudo-first order reaction:

$$-\frac{dC}{dt} = k_{CR}C$$

where, C is the concentration of CR dye at time t and k_{CR} is the first order degradation constant. In order to calculate this degradation constant, the absorbance of the CR dye sample at various time intervals was taken. The results were fitted to the previous model and the k_{CR} was calculated from the slope of the plot between ln $[C_o/C_f]$ and reaction time, t (Fig. 12). The degradation constant was found out to be

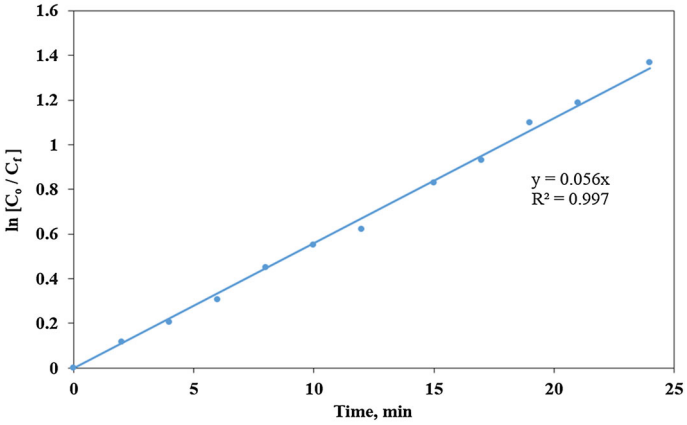

Fig. 12 First order degradation kinetics of CR dye in the presence of SNPs as catalyst

0.056 min^{-1}. Similar kind of studies was performed by [11] in which the CR dye was degraded within 15 min in the presence of SNPs prepared using *Amaranthus gangeticus* Linn leaf extract.

Conclusions

This study described the green synthesis of SNPs by using the fruit extract of *Bridelia retusa*. The method given in this study is very rapid and devoid of any harmful chemical which endorses the eco-friendliness and green nature. The synthesised nanoparticles were characterized by various methods which endorsed the nano range of the particles. The synthesised nanoparticles were found to a have high catalytic effect in degrading the Congo red dye and therefore these green nanoparticles could play a vital role in the development of novel nanocatalysts. The anticoagulant activity of the SNPs was successfully demonstrated which may find applications in the field of nanomedicines for the treatment of blood coagulation disorders.

Acknowledgements The contributors thankfully acknowledge the Department of Biotechnology, Manipal Institute of Technology (MIT), Manipal University for providing all the facilities to perform the research work.

Compliance with Ethical Standards

Conflict of interests The contributors declare that they do not have any conflict of interests.

References

1. K. Venugopal, et al. (2016). Synthesis of silver nanoparticles (Ag NPs) for anticancer activities (MCF 7 breast and A549 lung cell lines) of the crude extract of *Syzygium aromaticum*. *J. Photochem. Photobiol. B Biol.* **167**, 282–289.
2. V. Kumar, D. K. Singh, S. Mohan, R. K. Gundampati, and S. H. Hasan (2017). Photoinduced green synthesis of silver nanoparticles using aqueous extract of *Physalis angulata* and its antibacterial and antioxidant activity. *J. Environ. Chem. Eng.* **5**, 744–756.
3. A. Lateef, S. A. Ojo, and S. M. Oladejo (2016). Anti-candida, anti-coagulant and thrombolytic activities of biosynthesized silver nanoparticles using cell-free extract of *Bacillus safensis* LAU 13. *Process Biochem.* **51**, (10), 1406–1412.
4. E. E. Elemike, D. C. Onwudiwe, A. C. Ekennia, R. C. Ehiri, and N. J. Nnaji (2017). Phytosynthesis of silver nanoparticles using aqueous leaf extracts of *Lippia citriodora*: antimicrobial, larvicidal and photocatalytic evaluations. *Mater. Sci. Eng. C* **75**, 980–989.
5. M. N. M. Cunha, H. P. Felgueiras, I. Gouveia, and A. Zille (2017). Synergistically enhanced stability of laccase immobilized on synthesized silver nanoparticles with water-soluble polymers. *Colloids Surfaces B Biointerfaces* **154**, 210–220.
6. B. Sinduja and S. A. John (2017). Ultrasensitive optical sensor for hydrogen peroxide using silver nanoparticles synthesized at room temperature by GQDs. *Sens. Actuators B Chem.* **247**, 648–654.
7. K. Tahir, et al. (2015). An efficient photo catalytic activity of green synthesized silver nanoparticles using *Salvadora persica* stem extract. *Sep. Purif. Technol.* **150**, 316–324.
8. B. Kumari and D. P. Singh (2016). A review on multifaceted application of nanoparticles in the field of bioremediation of petroleum hydrocarbons. *Ecol. Eng.* **97**, 98–105.

9. V. A. Litvin, R. L. Galagan, and B. F. Minaev (2012). Colloids and surfaces A: physicochemical and engineering aspects kinetic and mechanism formation of silver nanoparticles coated by synthetic humic substances. *Colloids Surfaces A Physicochem. Eng. Asp.* **414**, 234–243.
10. R. M. Kumari, N. Thapa, N. Gupta, A. Kumar, and S. Nimesh (2016). Antibacterial and photocatalytic degradation efficacy of silver nanoparticles biosynthesized using *Cordia dichotoma* leaf extract. *Adv. Nat. Sci. Nanosci. Nanotechnol.* **7**, (4), 45009.
11. H. Kolya, P. Maiti, A. Pandey, and T. Tripathy (2015). Green synthesis of silver nanoparticles with antimicrobial and azo dye (Congo red) degradation properties using *Amaranthus gangeticus* Linn leaf extract. *J. Anal. Sci. Technol.* **6**, (1), 33–39.
12. S. Hamedi, S. Abbas, and A. Mohammadi (2017). Evaluation of the catalytic, antibacterial and antibio fi lm activities of the *Convolvulus arvensis* extract functionalized silver nanoparticles. *J. Photochem. Photobiol. B Biol.* **167**, 36–44.
13. J. Lee, et al. (2017). Physiological and molecular plant pathology A novel photo-biological engineering method for *Salvia miltiorrhiza*—Mediated fabrication of silver nanoparticles using LED lights sources and its effectiveness against *Aedes aegypti* mosquito larvae and microbial pathogens. *Physiol. Mol. Plant Pathol.* 1–9.
14. V. Ravichandran, S. Vasanthi, S. Shalini, S. Adnan, and A. Shah (2016). Green synthesis of silver nanoparticles using *Atrocarpus altilis* leaf extract and the study of their antimicrobial and antioxidant activity. *Mater. Lett.* **180**, 264–267.
15. A. K. Owk and M. N. Lagudu (2016). *Bridelia retusa* (L.) Spreng. Fruits: antimicrobial efficiency and their phytochemical constituents. *Not. Sci. Biol.* **8**, (1), 33–36.
16. S. K. M. S. Malhotra (1973). Some useful and medicinal plants of Chandrapur district (Maharashtra State). *Bull. Bot. Surv. India* **15**, 13–21.
17. T. Kumar and V. Jain (2014). Antinociceptive and anti-inflammatory activities of bridelia retusa methanolic fruit extract in experimental animals. *Sci. World J.* **2014**, 890151. doi:10.1155/2014/890151.
18. V. Ramesh, V. Thivaharan and S. Raja (2017). Green synthesis, structural characterization, and catalytic activity of silver nanoparticles stabilized with *Bridelia retusa* leaf extract. *Green Process. Synth*. doi:10.1515/gps-2016-0236.
19. S. Raja, V. Ramesh, and V. Thivaharan (2015). Antibacterial and anticoagulant activity of silver nanoparticles synthesised from a novel source-pods of *Peltophorum pterocarpum*. *J. Ind. Eng. Chem.* **29**, 257–264.
20. V. K. Vidhu and D. Philip (2014). Spectroscopic, microscopic and catalytic properties of silver nanoparticles synthesized using *Saraca indica* flower. *Spectrochim. Acta Part A Mol. Biomol Spectrosc.* **117**, 102–108.
21. S. Phongtongpasuk, S. Poadang, and N. Yongvanich (2016). Environmental-friendly method for synthesis of silver nanoparticles from dragon fruit peel extract and their antibacterial activities. *Energy Proced.* **89**, 239–247.
22. S. Gul, et al. (2016). Novel synthesis of silver nanoparticles using melon aqueous extract and evaluation of their feeding deterrent activity against housefly *Musca domestica*. *Asian Pac. J. Trop. Dis.* **6**, (4), 311–316.
23. S. Eustis and M. A. El-Sayed (2006). Why gold nanoparticles are more precious than pretty gold: noble metal surface plasmon resonance and its enhancement of the radiative and nonradiative properties of nanocrystals of different shapes. *Chem. Soc. Rev.* **35**, (3), 209–217.
24. A. Ahmad, et al. (2016). *Isatis tinctoria* mediated synthesis of amphotericin B-bound silver nanoparticles with enhanced photoinduced antileishmanial activity: a novel green approach. *J. Photochem. Photobiol. B Biol.* **161**, 17–24.
25. S. Ahmed, M. Saifullah, M. Ahmad, B. L. Swami, and S. Ikram (2016). Green synthesis of silver nanoparticles using *Azadirachta indica* aqueous leaf extract. *J. Radiat. Res. Appl. Sci.* **9**, (1), 1–7.
26. M. F. Zayed, W. H. Eisa, Y. K. Abdel-Moneam, S. M. El-kousy, and A. Atia (2015). *Ziziphus spina-christi* based bio-synthesis of Ag nanoparticles. *J. Ind. Eng. Chem.* **23**, 50–56.
27. B. Kumar, K. Smita, L. Cumbal, and A. Debut (2016). Ficus carica (Fig) fruit mediated green synthesis of silver nanoparticles and its antioxidant activity: a comparison of thermal and ultrasonication approach. *Bionanoscience* **6**, (1), 15–21.
28. A. Saravanakumar, M. Ganesh, J. Jayaprakash, and H. T. Jang (2015). Biosynthesis of silver nanoparticles using *Cassia tora* leaf extract and its antioxidant and antibacterial activities. *J. Ind. Eng. Chem.* **28**, 277–281.

29. D. Mubarakali, N. Thajuddin, K. Jeganathan, and M. Gunasekaran (2011). Plant extract mediated synthesis of silver and gold nanoparticles and its antibacterial activity against clinically isolated pathogens. *Colloids Surfaces B Biointerfaces* **85**, (2), 360–365.
30. T. V. M. Sreekanth, S. Ravikumar, and I. Y. Eom (2014). Green synthesized silver nanoparticles using *Nelumbo nucifera* root extract for efficient protein binding, antioxidant and cytotoxicity activities. *J. Photochem. Photobiol. B Biol.* **141**, 100–105.
31. W. Zhang, Z. Chen, H. Liu, L. Zhang, P. Gao, and D. Li (2011). Biosynthesis and structural characteristics of selenium nanoparticles by *Pseudomonas alcaliphila*. *Colloids Surfaces B Biointerfaces* **88**, (1), 196–201.
32. N. Saha, P. Trivedi, and S. D. Gupta (2016). Surface plasmon resonance (SPR) based optimization extract of *Curculigo orchioides* gaertn. and Its. *J. Clust. Sci.* **27**, (6), 1893–1912.
33. V. A. Litvin and B. F. Minaev (2014). The size-controllable, one-step synthesis and characterization of gold nanoparticles protected by synthetic humic substances. *Mater. Chem. Phys.* **144**, (1–2), 168–178.
34. S. Rajeshkumar, C. Malarkodi, M. Vanaja, and G. Annadurai (2016). Anticancer and enhanced antimicrobial activity of biosynthesizd silver nanoparticles against clinical pathogens. *J. Mol. Struct.* **1116**, 165–173.
35. S. Raja, V. Ramesh, and V. Thivaharan (2017). Green biosynthesis of silver nanoparticles using *Calliandra haematocephala* leaf extract, their antibacterial activity and hydrogen peroxide sensing capability. *Arab. J. Chem.* **10**, (2), 253–261.
36. S. V. Patil, H. P. Borase, C. D. Patil, and B. K. Salunke (2012). Biosynthesis of silver nanoparticles using latex from few euphorbian plants and their antimicrobial potential. *Appl. Biochem. Biotechnol.* **167**, (4), 776–790.
37. A. R. Shahverdi, S. Minaeian, H. R. Shahverdi, H. Jamalifar, and A. A. Nohi (2007). Rapid synthesis of silver nanoparticles using culture supernatants of *Enterobacteria*: a novel biological approach. *Process Biochem.* **42**, (5), 919–923.
38. J. S. Almeida, F. Lima, S. Da Ros, L. O. S. Bulhões, L. M. de Carvalho, and R. C. R. Beck (2010). Nanostructured systems containing rutin. In vitro antioxidant activity and photostability studies. *Nanoscale Res. Lett.* **5**, (10), 1603–1610.
39. T. C. Prathna, N. Chandrasekaran, A. M. Raichur, and A. Mukherjee (2011). Kinetic evolution studies of silver nanoparticles in a bio-based green synthesis process. *Colloids Surfaces A Physicochem. Eng. Asp.* **377**, (1–3), 212–216.
40. M. Sathishkumar, K. Sneha, S. W. Won, C. W. Cho, S. Kim, and Y. S. Yun (2009). *Cinnamon zeylanicum* bark extract and powder mediated green synthesis of nano-crystalline silver particles and its bactericidal activity. *Colloids Surfaces B Biointerfaces* **73**, (2), 332–338.
41. S. Shrivastava, T. Bera, S. K. Singh, G. Singh, P. Ramachandrarao, and D. Dash (2009). Characterization of antiplatelet properties of sivler nanoparticles. *ACS Nano* **3**, (6), 1357–1364.
42. V. A. Sakkas, M. A. Islam, C. Stalikas, and T. A. Albanis (2010). Photocatalytic degradation using design of experiments: a review and example of the Congo red degradation. *J. Hazard. Mater.* **175**, (1–3), 33–44.
43. B. Ajitha, Y. Ashok Kumar Reddy, S. Shameer, K. M. Rajesh, Y. Suneetha, and P. Sreedhara Reddy (2015). *Lantana camara* leaf extract mediated silver nanoparticles: antibacterial, green catalyst. *J. Photochem. Photobiol. B Biol.* **149**, 84–92.